Supporting Information

Huo et al. 10.1073/pnas.1000743107

SI Experimental Procedures

Plasmids, Cell Culture, and Transfection. Construction of myc-tagged EGFR/EGFR$_{mNLS}$ plasmids, piNOS-Luc, and cyclin D1 promoter plasmid with either wild-type ATRS or mutant ATRS were previously described (1–4).

RHA was amplified from the cDNA of HeLa cells and subcloned into a p3×Flag-CMV10 vector. GST-RHA fusion proteins were prepared using a standard protocol. The interference RNA sequences used in this study were RHA siRNA: 5′-GCAUAAAACUUCUGCGUCU-3′ (5), RHA shRNA (pLKO-1-DHX9): 5′-GGCTTTCGTTTAATACAATAG-3′ (3′-UTR), AllStars Negative Control siRNA (Qiagen) and nontarget control shRNA (pLKO-1-TRC, Addgene).

Cellular Fractionation, Western Blot, and ChIP. Cellular fractionation and western blot were performed as described previously (2). Antibodies used in this study were antibodies against EGFR (NeoMarkers/Santa Cruz), lamin B (Calbiochem), RHA (Abcam), a-tubulin, myc and flag (Sigma), and cyclin D1 (Cell Signaling). All secondary antibodies were obtained from Sigma. Chromatin Immunoprecipitation (ChIP) was performed as described previously (3, 4).

Luciferase Reporter Assay. HeLa cells were transfected with plasmid DNA for 6 h and treated with EGF (50 ng/ml) for 5 h before luciferase assay. A pβ-actin-Renilla promoter plasmid was cotransfected as internal control to correct transfection efficiency. The luciferase activities were presented as mean value ± SD.

Confocal Analysis and Immunohistochemical Staining. Confocal analysis of colocalization of EGFR and RHA was performed as described previously (2), and images were captured using Zeiss LSM 710 laser microscope. For immunohistochemical staining of human breast cancer tissue samples, each sample was stained with specific antibodies as indicated and scored using an H-score method combining the values of immunoreaction intensity and the percentage of tumor cell staining. Briefly, the immunoreactivity of EGFR, RHA, and cyclin D1 were classified into one of two groups according to the percentage of tumor cells positive for proteins: *i*) positive (+, >10%) or *ii*) negative (− and ±, <10%). Fifty-one surgically resected human breast cancer specimens were collected in the Department of Pathology at Shanghai East Breast Disease Hospital (Shanghai, China). The X^2 test was used to analyze the relationship among nuclear expression levels of EGFR, RHA, and cyclin D1 in these specimens. Statistical analysis was performed and graphs were created using SPSS software program, and P values <0.05 were considered statistically significant.

1. Hsu SC, Miller SA, Wang Y, Hung MC (2009) Nuclear EGFR is required for cisplatin resistance and DNA repair. *Am J Transl Res* 1(3):249–258.
2. Hsu SC, Hung MC (2007) Characterization of a novel tripartite nuclear localization sequence in the EGFR family (Translated from English). *J Biol Chem* 282(14):10432–10440.
3. Lin SY, et al. (2001) Nuclear localization of EGF receptor and its potential new role as a transcription factor (Translated from English). *Nat Cell Biol* 3(9):802–808.
4. Lo HW, et al. (2005) Nuclear interaction of EGFR and STAT3 in the activation of the iNOS/NO pathway (Translated from English). *Cancer Cell* 7(6):575–589.
5. Tetsuka T, et al. (2004) RNA helicase A interacts with nuclear factor kappaB p65 and functions as a transcriptional coactivator (Translated from English). *Eur J Biochem* 271 (18):3741–3751.

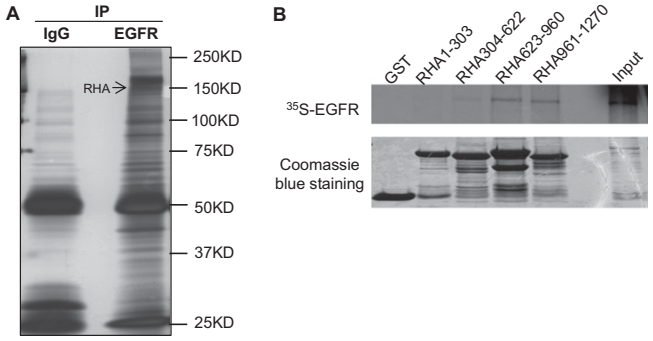

Fig. S1. (*A*) Silver staining of proteins associated with nuclear EGFR. Nuclear proteins from A431 cells were used for immunoprecipitation (IP) and MS. The arrow indicates the potential band for RHA. (*B*) Direct interaction between EGFR and RHA in vitro. (*Upper*) In vitro transcribed and translated [^{35}S]Met-labeled EGFR was incubated with recombinant GST-RHA fragments, pulled down using glutathione-Sepharose beads, separated by SDS/PAGE, and visualized using autoexposure. (*Lower*) The same protein gel stained with Coomassie blue is shown as loading control.

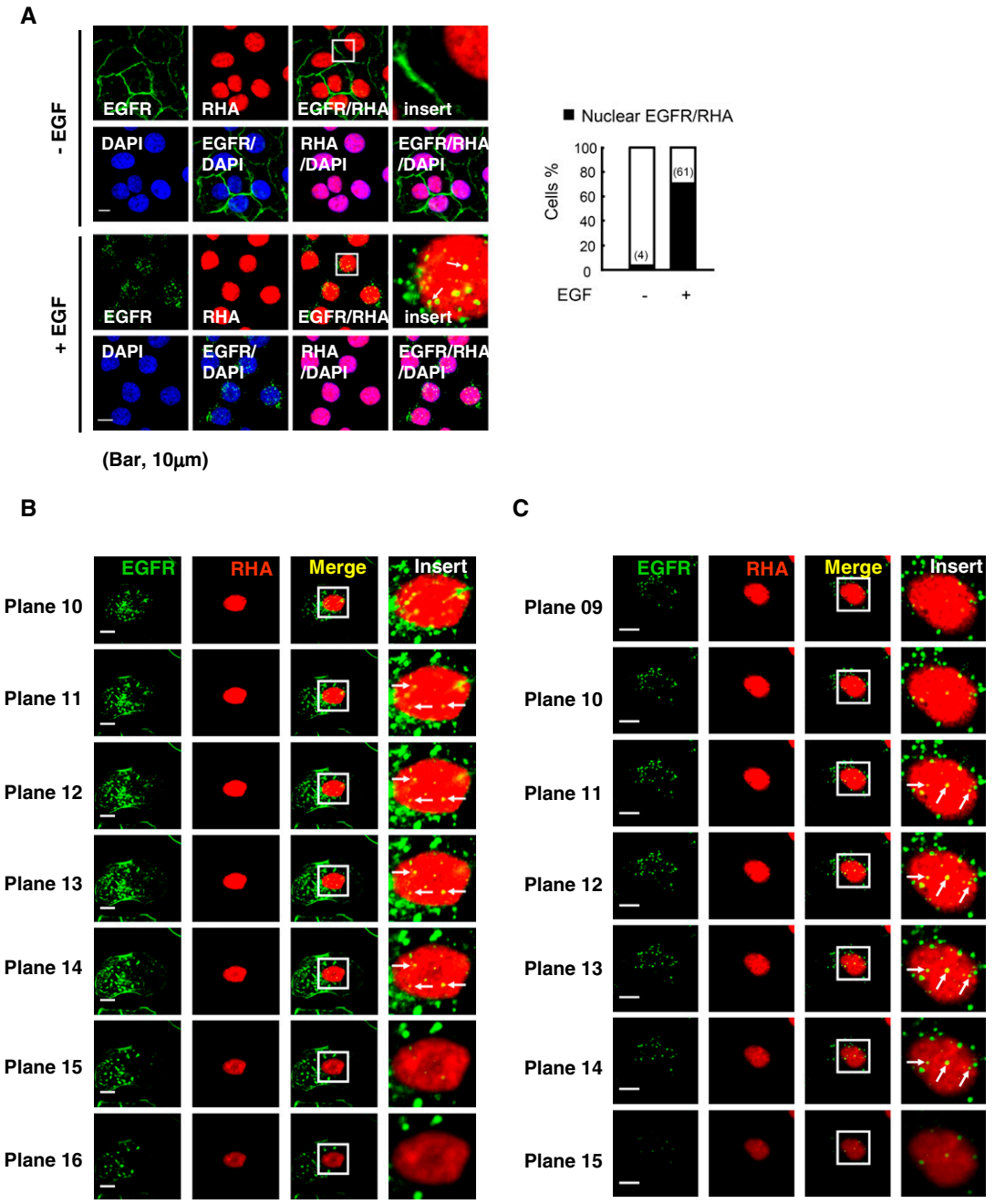

Fig. S2. Colocalization of EGF receptor (EGFR) and RNA helicase A (RHA) in HeLa cells and MDA-MB-468 cells. (*A*) (*Left*) Colocalization of EGFR and RHA in HeLa cells. HeLa cells were serum starved overnight and then treated with EGF (50 ng/mL, 30 min) or not treated, fixed with paraformaldehyde, and stained with anti-EGFR and anti-RHA antibodies. Colocalization of EGFR and RHA is shown in the yellow merged image (arrows). (*Right*) The percentage of cells with colocalization of EGFR and RHA was calculated in 50 counted cells and is shown in the bar graph. (*B*) Serial focal sections of an MDA-MB-468 cell Indicating nuclear colocalization of EGFR and RHA. MDA-MB-468 cells were fixed with paraformaldehyde and stained with anti-EGFR and anti-RHA antibodies. A single cell was dissected into 27 focal sections, each 0.5 μm thick. The nucleus spanned focal planes 6–19, and the RHA/EGFR complex is shown clearly from plane 11–14 in the merged images (arrows in *Inset*). The images were captured using a Zeiss LSM 710 laser microscope. (Scale bar, 10 μm.) (*C*) Serial focal sections of a HeLa cell indicating nuclear colocalization of EGFR and RHA. HeLa cells were fixed with paraformaldehyde and stained with anti-EGFR and anti-RHA antibodies. A single cell was dissected into 22 focal sections, each 0.5 μm thick. The nucleus spanned focal planes 5–17, and the RHA/EGFR complex is shown clearly from plane 11–14 in the merged images (arrows in *Inset*). The images were captured using a Zeiss LSM 710 laser microscope. (Scale bar, 10 μm.)

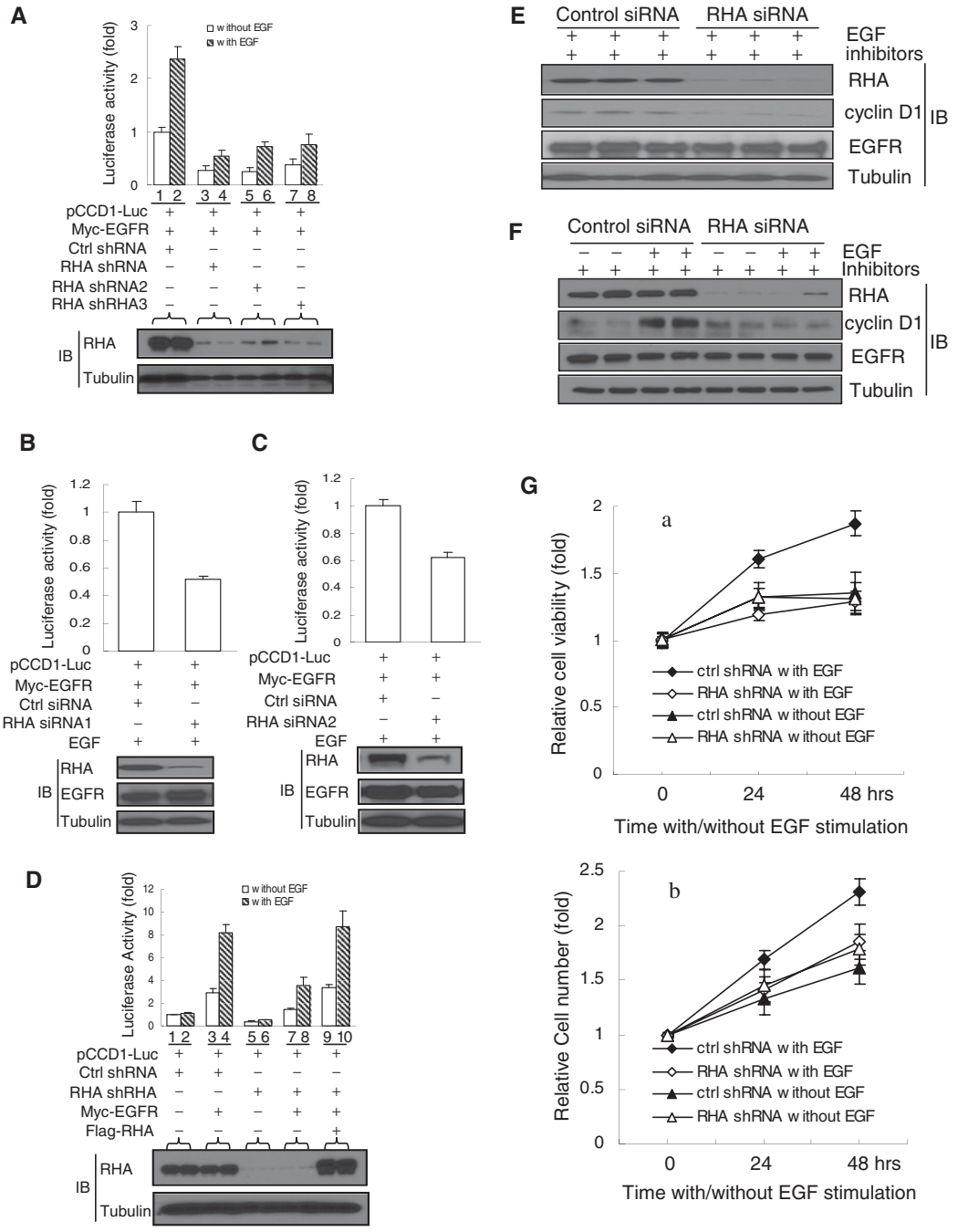

Fig. S3. Reduction of EGF/EGFR-induced cyclin D1 gene expression by knockdown of RHA expression. (*A*) EGF/EGFR-induced cyclin D1 promoter activity is reduced in HeLa cells with stable expression of shRNAs targeting different regions of RHA mRNA. HeLa cells were stably transfected with control shRNA (nontargeting sequence: 5′-CCGCAGGTATGCACGCGT-3′), RHA shRNA targeting the 3′-UTR of RHA mRNA (5′-GGCTTTCGTTTAATACAATAG-3′), RHA shRNA2 targeting the coding region of RHA mRNA (5′-GAAGGATTACTACTCAAGAAA-3′), and RHA shRNA3 targeting another coding region of RHA mRNA (5′-TCGAGGAATCAGTCATGTAAT-3′). The stable clone cells were transiently transfected with cyclin D1 promoter construct (pCCD1-Luc, β-actin promoter-Renilla reporter construct, and Myc-tagged EGFR plasmid) and then were serum starved overnight followed by treatment with EGF (50 ng/mL) for 5 h or no treatment. Luciferase activity was measured according to standard procedures. The data are presented as the mean results ± SD (n = 3). The expression levels of RHA in these cells are shown by Western blot. IB, immunoblotting. (*B*) EGFR-induced cyclin D1 promoter activity is reduced by transient knockdown of RHA using RHA siRNA1 in HeLa cells. HeLa cells were transiently transfected with either control (Ctrl) siRNA (AllStars Negative Control siRNA; Qiagen) or RHA siRNA1 (targeting sequence: 5′-AAGAAGUGCAAGCGACUCUAG-3′) previously reported by Zhong et al. (1). (*C*) EGFR-induced cyclin D1 promoter activity is reduced by transient knockdown of RHA using RHA siRNA2 in HeLa cells. HeLa cells were transiently transfected with control siRNA (AllStars Negative Control siRNA; Qiagen) or RHA siRNA2 (targeting sequence: 5′-GCAUAAAACUUCUGCGUCU-3′) previously reported by Tetsuka et al. (2). Luciferase activity was measured as described above. (*D*) Down-regulation of cyclin D1 promoter activity in HeLa cells with stable expression of RHA shRNA can be rescued by reexpression of RHA. HeLa cells with stable expression of RHA shRNA targeting the region at 3′-UTR of RHA mRNA were transfected by the indicated plasmids. Luciferase activity was measured as described in Fig. S3*A*. The expression levels of RHA and tubulin (loading control) are shown by Western blot in the lower panel. (*E*) Knockdown of RHA expression reduces EGF/EGFR-induced endogenous cyclin D1 gene expression in HeLa cells. HeLa cells were transfected with control siRNA or RHA siRNA1 for 24 h and then were transfected with Myc-tagged EGFR. (Each siRNA-based experiment was conducted in triplicate.) Forty-eight hours after siRNA transfection, cells

Legend continued on following page

were serum starved overnight and then were treated for 5 h with EGF (50 ng/mL) combined with inhibitors of three major known EGFR traditional downstream signal pathways (10 μM LY294002, 10 μM U0126, and 10 μM staurosporine to inhibit PI3K, MAPK, and protein kinase C, respectively). Cells then were subjected to lysis and immunoblotting with defined specific antibodies. (*F*) Knockdown of RHA expression reduces EGF/EGFR-induced endogenous cyclin D1 gene expression in A431 cells. A431 cells were transfected with control or RHA siRNA1 using electroporation. Forty-eight hours after transfection, cells were serum starved overnight and then were treated for 5 h with the three inhibitors of known EGFR downstream signaling pathways as described in Fig. S3*E* with or without 50 ng/mL EGF. (For each treatment, experiments were performed in duplicate.) Cells then were subjected to lysis for Western blotting to determine the cyclin D1, RHA, EGFR, and α-tubulin expression levels. (*G*) Knocking down RHA slows cell growth. (*Upper*) MTT assay was used to monitor the proliferation of HeLa cells with stable-expressing control shRNA and RHA shRNA. Equal amounts of cells were seeded on six-well plates overnight followed by serum starvation for 15 h. The cells were stimulated without or with 50 ng/mL EGF for different time periods. Cell growth with different durations of EGF stimulation was monitored by MTT assay. (*Lower*) Cell growth was measured by counting cell numbers at different durations of EGF stimulation. Equal amounts of cells were seeded in each well in six-well plates. (Each treatment was performed in triplicate.) After overnight serum starvation, cells were treated or not treated with 50 ng/mL EGF for different time durations, and cell numbers from each treatment were counted.

1. Zhong X, Safa AR. (2004) RNA helicase A in the MEF1 transcription factor complex up-regulates the MDR1 gene in multidrug-resistant cancer cells. *J Biol Chem* 279(17):17134–17141.
2. Tetsuka T et al. (2004) RNA helicase A interacts with nuclear factor kappaB p65 and functions as a transcriptional coactivator. *Eur J Biochem* 271(18):3741–3751.

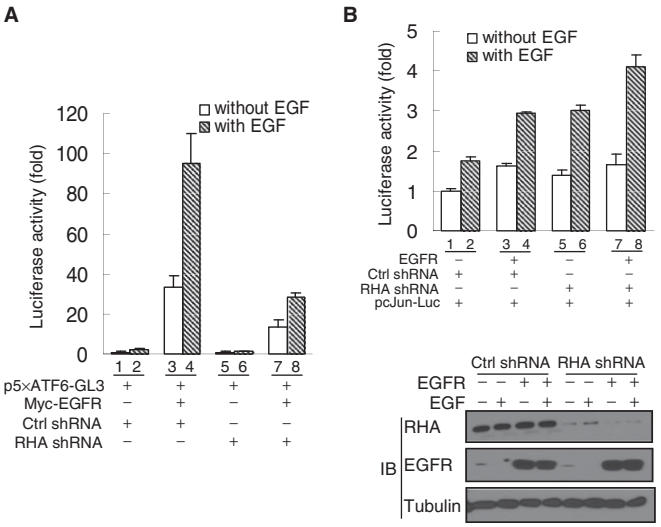

Fig. S4. Effects of knocking down RHA on EGFR-induced c-fos and c-Jun promoter activities. (*A*) Knocking down RHA reduces EGFR-induced c-fos promoter activity. HeLa cells were transfected by the indicated plasmids. Cells were treated with EGF (50 ng/mL) for 5 h after overnight serum starvation or were left untreated. Luciferase assay was performed, and data are presented as the mean results ± SD ($n = 3$). p5×ATF6-GL3 plasmid (1) containing the minimal human c-fos promoter (−53 to +45) with the AT-rich sequence (ATRS) EGFR binding sequence was purchased from Addgene. (*B*) Knocking down RHA does not reduce c-Jun promoter activity. The experiment in Fig. S4*B* was performed in HeLa cells using pcJun-Luc promoter constructs instead of the c-fos promoter construct.

1. Wang Y, et al. (2000) Activation of ATF6 and ATF6 DNA binding site by the endoplasmic reticulum stress response. *J Biol Chem* 275:27013–27020.

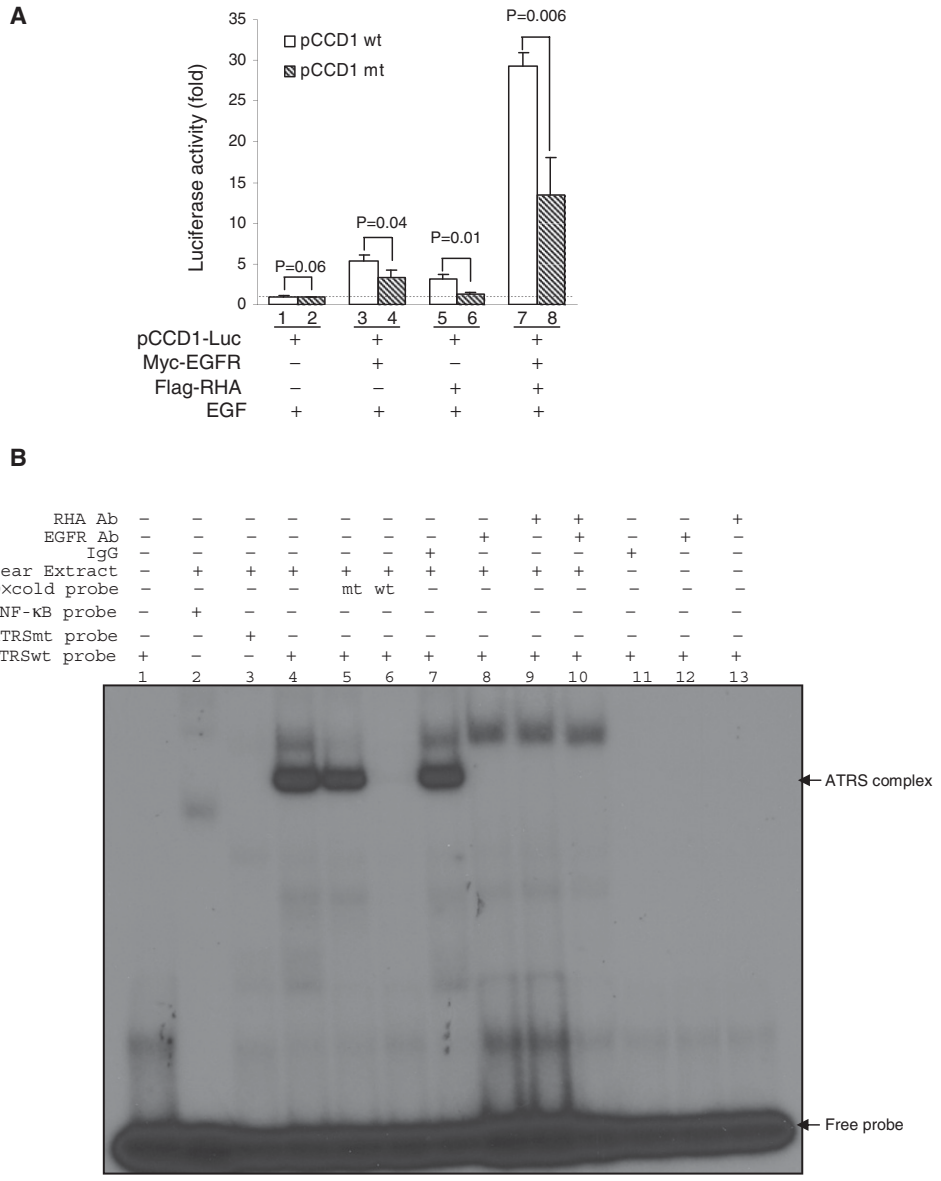

Fig. S5. ATRS-dependent regulation of gene expression by the EGFR/RHA complex. (*A*) ATRS-dependent activation of the cyclin D1 promoter by EGFR and RHA. HeLa cells transfected with the indicated plasmids were serum starved and treated with EGF for 5 h before a luciferase assay was performed. The *P* values calculated from the *t* test are shown above each pair of bars (replotted from Fig. 2*C*). mt, mutation; wt, wild-type. (*B*) EMSA indicating that the EGFR/RHA protein complex binds specifically to a DNA probe containing an ATRS. Nuclear lysates (10–15 μg) extracted from EGF-treated A431 cells were incubated with 10^5 cpm of ATRS probe (1) for 20 min at room temperature followed by electrophoresis in a 5% nondenaturing gel and exposure at −80 °C for 4 h after gel-drying. In the competition experiments, a 50-fold excess of cold probes was incubated with 10–15 μg nuclear lysates for 20 min at room temperature. Antibodies to EGFR [1 μg sc-03 (Santa Cruz) and 1 μg Ab-13 (Neomarkers)] and RHA (3 μg ab26271; Abcam) or normal IgG were used in the supershift experiments.

1. Lin SY et al. (2001) Nuclear localization of EGF receptor and its potential new role as a transcription factor. *Nat Cell Biol* 3:802–808.

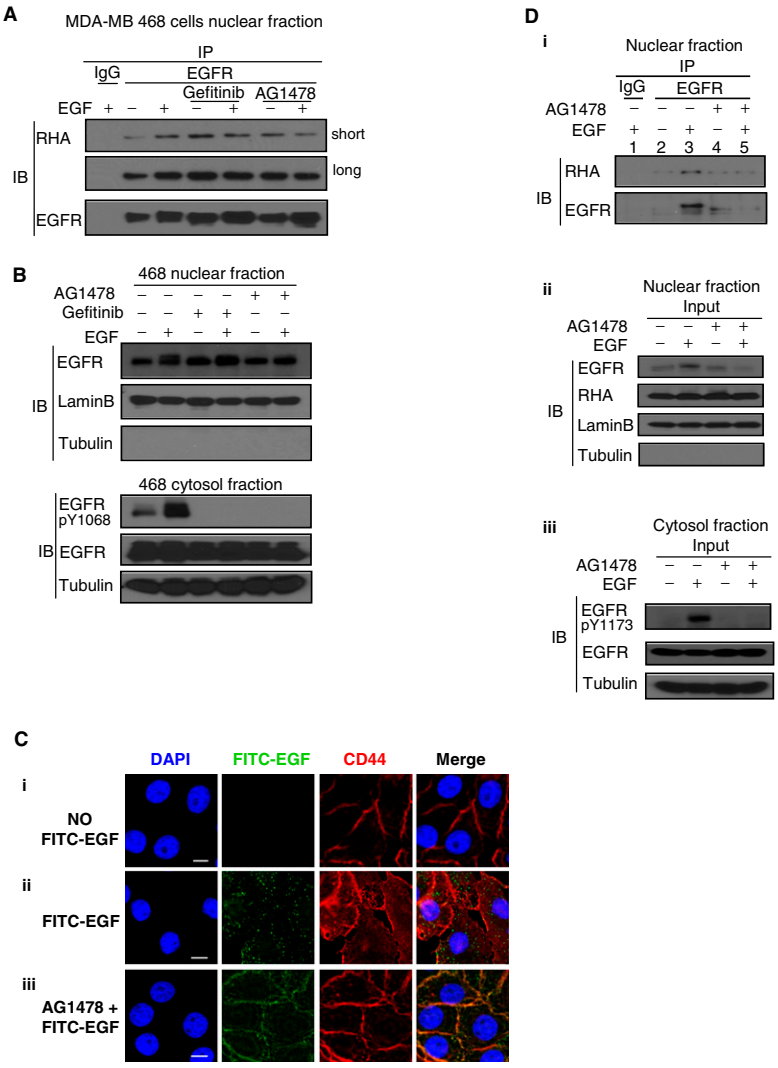

Fig. S6. Effect of EGFR tyrosine kinase inhibitor on EGF/EGFR internalization and the association of EGFR with RHA. (*A*) Effects of EGFR tyrosine kinase inhibitor on the interaction of EGFR with RHA in MDA-MB-468 cells. MDA-MB-468 cells serum starved overnight were treated or not treated with 50 ng/mL EGF alone or together with pretreatment for 30 min with either Gefitinib (10 μM) or AG1478 (10 μM). Cells were collected and fractionated. Nuclear fractionation was immunoprecipitated by anti-EGFR antibody or by normal IgG. The immunoprecipitates were used for Western blot to detect the RHA with anti-RHA antibody. The same membrane reblotted with anti-EGFR antibody after stripping is shown for the EGFR levels in the immunoprecipitates. (*B*) Effect of tyrosine kinase inhibitors on EGFR nuclear translocation in MDA-MB-468 cells. Cells were serum starved overnight, then were treated or not treated with tyrosine kinase inhibitors (Gefitinib/AG1478, 10 μM) for 30 min, and then were stimulated or not stimulated by 50 ng/mL EGF for 30 min before cell collection and fractionation. Equal amounts of nuclear fraction from each sample were loaded for Western blot to detect the expression level of EGFR. The same membrane reblotted with anti-lamin B and anti-tubulin antibodies is shown as the loading control and fractionation control. The cytosol fraction of the cells used to detect the level of EGFR.Y1068 phosphorylation after the treatment indicates that the tyrosine kinase inhibitors are effective in this study. (*C*) Effect of EGFR tyrosine kinase inhibitor on EGF internalization in HeLa cells. HeLa cells were serum starved overnight, then were pretreated with AG1478 pretreatment for 30 min or were left untreated, and then were treated with 50 ng/mL FITC-EGF for 5 min followed by washing and immunofluorescence confocal microscopy. CD44, cell membrane marker. (Scale bar: 5 μm.) (*D*) Effect of EGFR tyrosine kinase inhibitor on the association of endogenous EGFR with RHA in HeLa cells. HeLa cells were serum starved overnight and then were treated or were not treated with 50 ng/mL EGF for 30 min, with or without pretreatment of EGFR tyrosine kinase inhibitor for 30 min. Cells then were lysed and fractionated. (*Top*) Nuclear fractions were used for immunoprecipitation with anti-EGFR antibody followed by immunoblotting to detect RHA and EGFR. (*Middle*) Input of the nuclear fraction was used for immunoblotting to detect the expression levels of EGFR, RHA, lamin B, and α-tubulin in the nucleus of HeLa cells. (*Bottom*) Input from cytosol fraction was used to show the inhibitory effects of AG1478 on EGFR phosphorylation by blotting with anti-phosphorylated EGFR (pY1173) antibody.

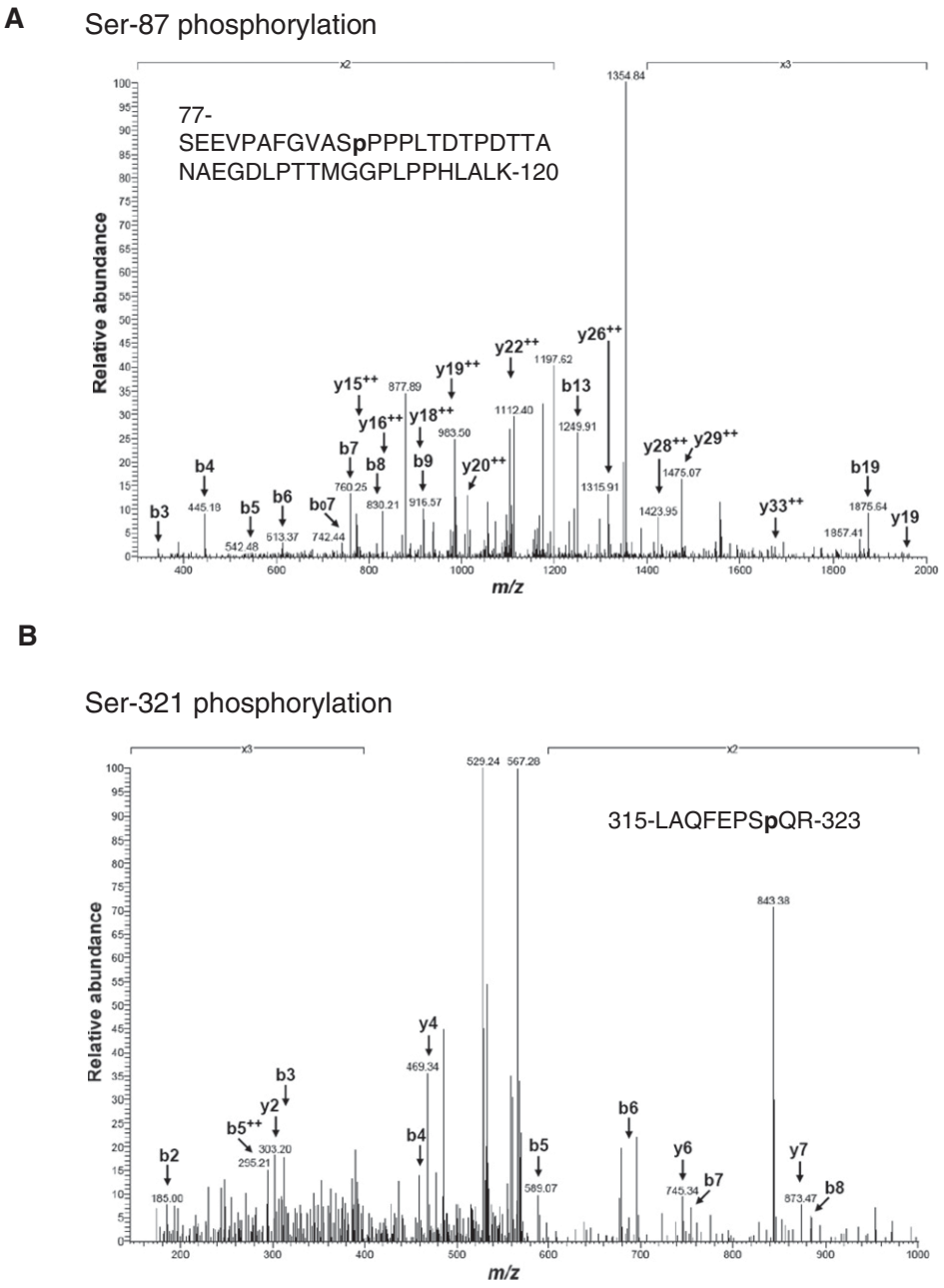

Fig. S7. MS analysis of phosphorylation of RHA. HEK293T cells were cotransfected with Flag-RHA and Myc-EGFR and stimulated with EGF (50 ng/mL) for 30 min after overnight serum starvation. Total lysate from the treated HEK293T cells was immunoprecipitated with an anti-Flag antibody and captured using protein A agarose beads. After extensive washing, the proteins pulled down by the antibody were resolved on an 8% SDS/PAGE, excised, and submitted to MS analysis for tyrosine/serine/threonine phosphorylation residues of RHA.

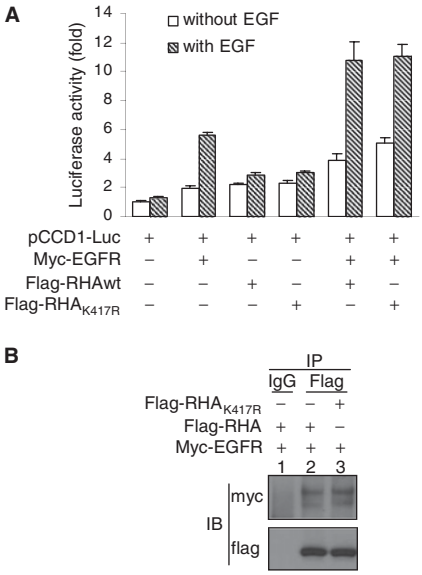

Fig. S8. **Effect of** RNA helicase-independent activity of RHA on its interaction with EGFR and on the transactivation of the cyclin D1 promoter. (*A*) Helicase activity of RHA-independent activation of EGFR/RHA-induced cyclin D1 promoter activity. HeLa cells transfected with the indicated plasmid were serum starved overnight and were treated with 50 ng/mL EGF for 5 h or were left untreated before luciferase assay. Data are shown as means ± SD (n = 3). (*B*) Helicase activity-independent interaction of RHA with EGFR in vivo. HEK293T cells were cotransfected with the indicated plasmids (Myc-EGFR together with either Flag-RHA or Flag-RHA$_{K417R}$) for 24 h, and total lysate was immunoprecipitated with either anti-Flag antibody or mouse IgG followed by immunoblotting to detect EGFR and RHA.

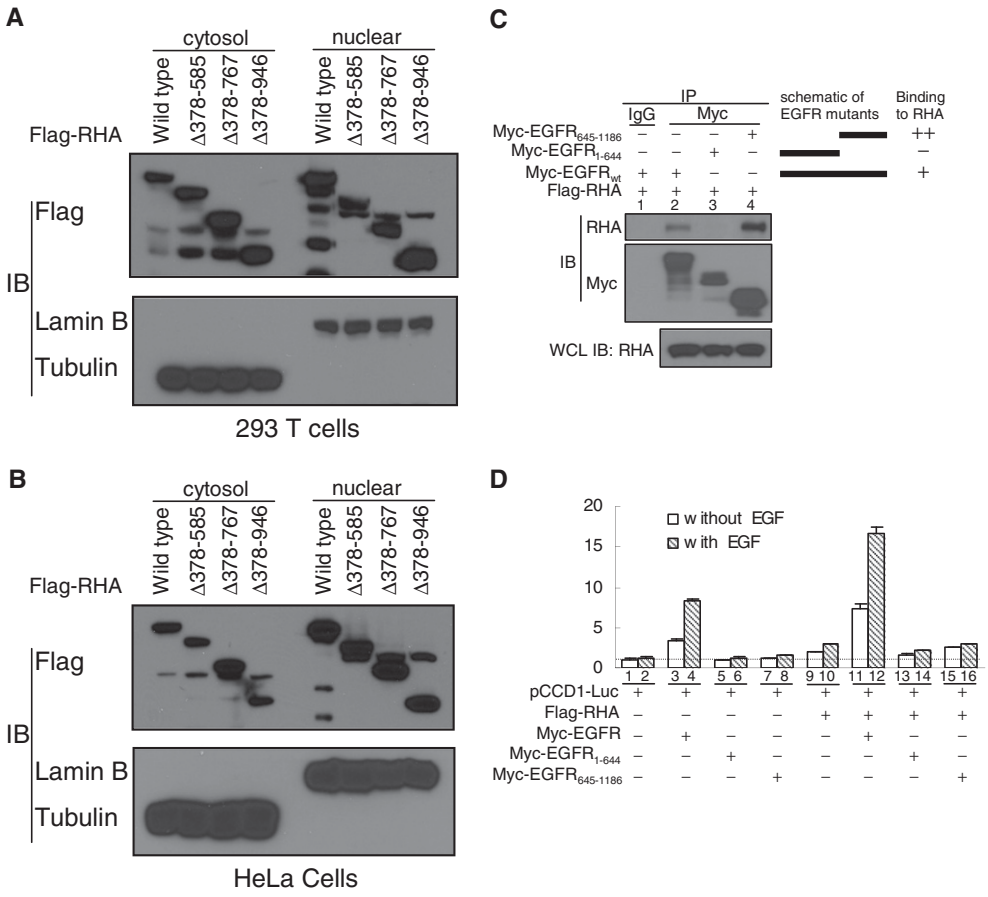

Fig. S9. Nuclear translocation of RHA mutants with helicase domain deletion (*A* and *B*) and reducing EGFR-induced cyclin D1 promoter activity by interruption of EGFR–RHA interaction (*C* and *D*). HEK293T (*A*) and HeLa (*B*) cells were transiently transfected with indicated RHA constructs for 24 h. Cells then were collected and fractionated followed by immunoblotting with anti-Flag antibody to detect the location of Flag-tagged RHA. The same membranes reblotted with anti-lamin B and anti-tubulin antibodies are shown as fractionation control. (*C*) Interaction between the intracellular domain of EGFR and RHA. HEK293T cells transfected with the indicated plasmids were lysed and immunoprecipitated with anti-Myc antibody followed by immunoblotting with anti-RHA antibody. The same membrane reblotted with anti-Myc antibody is shown as the loading control. The RHA expression level was shown by blotting the whole-cell lysate (WCL) with anti-RHA antibody. (*D*) Abrogation of EGFR/RHA-induced cyclin D1 promoter activity by EGFR deletion mutants. HeLa cells were transfected with the indicated plasmids. After overnight serum starvation, HeLa cells were treated with EGF (50 ng/mL) for 5 h or left untreated before luciferase assay. Data are shown as means ± SD (n = 3).

Table S1. Proteins associated with nuclear EGFR identified by mass spectrometry analysis

Accession no.	Protein name	Accession no.	Protein name
AAC52019	DNA-dependent protein kinase catalytic subunit (DNA-PK)		
O75643	U5 small nuclear ribonucleoprotein 200 kDa helicase	P55072	Transitional endoplasmic reticulum ATPase
Q15149	Plectin-1	NP_005057	Splicing factor, proline- and glutamine-rich
NP_112598	Epiplakin	NP_001952	Eukaryotic translation elongation factor 2
P49792	E3 SUMO-protein ligase RanBP2	NP_056473	Nucleolar complex associated 2 homolog
NP_004850	Clathrin heavy chain 1	Q9NXF1	Testis-expressed sequence 10 protein
NP_006436.3	PremRNA-processing-splicing factor 8	P08238	Heat shock protein HSP 90-beta
NP_079199	Nuclear pore membrane glycoprotein 210 precursor	Q14974	Importin subunit beta-1
NP_003118	Spectrin alpha chain, brain	EAW82887	Nuclear pore complex protein Nup93
NP_065182	THO complex subunit 2	NP_001349	DEAH (Asp-Glu-Ala-His) box polypeptide 15
NP_000928	DNA-directed RNA polymerase II subunit RPB1	NP_006730	Minichromosome maintenance complex component 5
NP_000929	DNA-directed RNA polymerase II subunit RPB2	Q99959	Plakophilin-2
NM_001357	ATP-dependent RNA helicase A (RHA)	NP_006830	Inner membrane protein, mitochondrial isoform 1
NP_055950	Nuclear pore complex protein Nup205		
CAI13775	HEAT repeat-containing protein 1	P14923	Junction plakoglobin (Catenin gamma)
NP_006176	Nuclear mitotic apparatus protein 1	NP_056189	Unc-84 homolog B
NP_056169	Nucleoporin NUP188 homolog	NP_009114	Plakophilin-3
NP_002636	Phosphatidylinositol-4-phosphate 3-kinase C2 domain-containing alpha polypeptide	AAC39540	Heterogeneous nuclear ribonucleoprotein R
O75533	Splicing factor 3B subunit 1	NP_066964	ATP-dependent DNA helicase II (86 kDa subunit of Ku antigen)
NP_006297	Structural maintenance of chromosomes protein 1A	NP_002874	Ran GTPase-activating protein 1
O60306	Intron-binding protein aquarius	NP_002851	Pyrroline-5-carboxylate synthetase isoform 1
Q9UDY2	Tight junction protein ZO-2	NP_001317	Cleavage stimulation factor subunit 3 isoform 1
NP_055204	Proline-, glutamic acid- and leucine-rich protein 1	NP_005234	Ewing sarcoma breakpoint region 1 isoform EWS
		NP_002477	Nuclear cap-binding protein subunit 1
NP_005436	Structural maintenance of chromosomes protein 3	NP_005959	Heterogeneous nuclear ribonucleoprotein M
Q12769	Nuclear pore complex protein Nup160	NP_005338	Heat shock 70kDa protein 5
Q8WVM7	Cohesin subunit SA-1	Q92841	Probable ATP-dependent RNA helicase DDX17
Q8N3U4	Cohesin subunit SA-2	NP_057291	Cleavage and polyadenylation specificity factor subunit 3
O75694	Nuclear pore complex protein Nup155	NP_005122	THO complex subunit 1
Q14126	Desmoglein-2 precursor	O15031	Plexin-B2 precursor (MM1)
P00505	Aspartate aminotransferase, mitochondrial precursor	NP_006588	Heat shock cognate 71 kDa protein (heat shock 70kDa protein 8 isoform 1)
Q13435	Splicing factor 3B subunit 2	NP_733821	Lamin-A/C
Q8WUM0	Nuclear pore complex protein Nup133	NP_005337	Heat shock 70 kDa protein 1 (heat shock 70kDa protein 1B)
O75400	PremRNA-processing factor 40 homolog A	NP_005564	Lamin-B1
		NP_004125	Heat shock 70kDa protein 9 precursor
		O00571	ATP-dependent RNA helicase DDX3X
NP_036558	Splicing factor 3B subunit 3	O60506	Heterogeneous nuclear ribonucleoprotein Q
Q15029	116 kDa U5 small nuclear ribonucleoprotein component	NP_001460	ATP-dependent DNA helicase II, 70 kDa subunit (70 kDa subunit of Ku antigen; Ku70)
O43795	Myosin-Ib	NP_006319	RNA-binding protein 14
Q00839	Heterogeneous nuclear ribonucleoprotein U	Q5BKZ1	Zinc finger protein 326 (zinc finger protein 326 isoform 1)
NP_056992	Arsenite-resistance protein 2 isoform a	Q9UBU9	Nuclear RNA export factor 1
NP_003950	Huntingtin-interacting protein 1-related protein	P35637	RNA-binding protein FUS
P22223	Cadherin-3 precursor (P-Cadherin)	NP_000235	Menin (menin isoform 1)
NP_112604	Heterogeneous nuclear ribonucleoprotein C isoform a	P04843	Dolichyl-diphosphooligosaccharide–protein glycosyltransferase 67 kDa subunit precursor
NP_066997	p30 DBC protein	NP_004387	Probable ATP-dependent RNA helicase DDX5
NP_056175	Superkiller viralicidic activity 2-like 2	NP_116126	Lamin-B2
Q68E01	Integrator complex subunit 3	NP_000468	Albumin preproprotein
P23229	Integrin alpha-6 precursor	NP_006550	Sam68, KH domain-containing, RNA-binding, signal transduction-associated protein 1
NP_075068	Nucleolar protein family 6 alpha isoform	P19525	IFN-induced, double-stranded RNA-activated protein kinase
NP_061322	Matrin-3	NP_055416	EH domain-containing protein 2
O00159	Myosin-Ic	NP_112552	Heterogeneous nuclear ribonucleoprotein K

Table S1. Cont.

Accession no.	Protein name	Accession no.	Protein name
NP_001073027	Heterogeneous nuclear ribonucleoprotein U-like protein 2	BAB18649	Heterogeneous nuclear ribonucleoprotein L
P57740	Nuclear pore complex protein Nup107	P04844	Dolichyl-diphosphooligosaccharide–protein glycosyltransferase 63 kDa subunit precursor
P52948	Nuclear pore complex protein Nup98-Nup96 precursor	P26368	Splicing factor U2AF 65 kDa subunit
P55265	Double-stranded RNA-specific adenosine deaminase	NP_036478	Nucleoporin 62kDa
P29590	Probable transcription factor PML	Q9NVI7	ATPase family AAA domain-containing protein 3A
NP_444513	Dermcidin preproprotein	Q9NVH1	DnaJ homolog subfamily C member 11
NP_003391	Exportin-1	NP_005424	Viral oncogene yes-1 homolog 1
NP_036387	5′-3′ exoribonuclease 2	Q9ULV4	Coronin-1C
P57678	Component of gems 4	NP_076983	Nucleolar complex protein 4 homolog
NP_036601	PRP6 premRNA processing factor 6 homolog	NP_036421	Kelch-like ECH-associated protein 1
Q9Y2U8	Inner nuclear membrane protein Man1	Q8IWJ2	GRIP and coiled-coil domain-containing protein 2
NP_006256	Double-strand-break repair protein rad21 homolog	P26599	Polypyrimidine tract-binding protein 1
NP_001093	Alpha-actinin-1	NP_031389	Non-POU domain-containing octamer-binding protein
NP_004915	Alpha-actinin-4	NP_002645	Pyruvate kinase, muscle isoform M2 (Pyruvate kinase isozymes M1/M2)
NP_001273	AP-2 complex subunit beta-1	NP_060615	Family with sequence similarity 82, member A2
O95782	AP-2 complex subunit alpha-1	Q08345	Epithelial discoidin domain-containing receptor 1 precursor
NP_036437	AP-2 complex subunit alpha-2	Q8IYB1	Uncharacterized protein C3orf59
NP_036350	Interleukin enhancer-binding factor 3 iso form a (ILF3) (NF90)	Q9BQE3	Tubulin alpha-1C chain
NP_001894	Catenin alpha-1 (Alpha E-catenin)	P42167	Lamina-associated polypeptide 2, isoforms beta/gamma
		AAB49972	SHC-transforming protein 1
Q96J02	E3 ubiquitin-protein ligase Itchy homolog	EAX04506	ubiquitin B, isoform CRA_e